
Fuel Cells and Hydrogen Joint Undertaking (FCH JU)

Project SMARTCat:

# WP2: D 2.1

# Report on the decoupling of strain, ligand and electronic effects in tri-metallic core-shell nanoparticles

Version 30/05/2014


## Content

**Authors:** Paul C. Jennings,[1] Vladimir Tripkovic,[2] Jon Steinar G. Myrdal,[1] Juan Maria Garcia-Lastra,[1] Jan Rossmeisl,[2] Tejs Vegge[1]

[1] Department of Energy Storage and Conversion, Technical University of Denmark (DTU), Denmark.

[2] Department of Physics, Technical University of Denmark (DTU), Denmark.

# 1 Introduction

Understanding and optimizing the relative contributions of strain and ligand effects is a critical aspect in the development of more active and stable Pt-based nanoalloy-catalysts for the Oxygen Reduction Reaction (ORR) [1]. Binary systems like PtAu, PtPd, PtNi, PtCo and PtY [2,3] have been shown to display high catalytic ORR activity, but retaining the structural composition and activity under operating conditions remains a challenge [4]. A third alloying element can be used to improve the stability, e.g. by limiting dissolution, but the catalytic consequences must also be understood.

Here, we have applied density functional theory (DFT) calculations in combination with linear scaling relations to establish ORR activity volcanoes as a function of well-established predictors like the oxygen and OH-binding energy relative to Pt, i.e. $\Delta E_{OH}$-$\Delta E^{Pt}_{OH}$, in the binary and tri-metallic Pt-Pd-Au systems [5,6]. We have investigated this system using a combination of model **thin-film structures** and 309-atom (2-3 nm) icosahedral **core-shell nanoparticles** in order to quantify to which extent changes in the catalytic activity can be attributed to strain and ligand effects in these systems.

## 1.1 Thin-film structures

We have investigated a range of possible near surface alloys and combinations of Pt, Pd and Au. For PtPd, we have analyzed structures with both Pt and Pd in the bulk and the surface composition is varied in the two topmost layers. For AuPt and AuPd, Pt was consistently used in the bulk, whereas the surface composition was varied between Pt and Au, and Pd and Au. The periodicity of the cell is $\sqrt{3}$ x $\sqrt{3}$, meaning there are three surface atoms in the unit cell (figure 1a). This limits the number of possible combination to $4^2$ and the ratios of alloy components in a single layer to 3:0, 2:1,1:2 and 0:3.

We have calculated the segregation energies of Au in the Pt and Pd matrix. Since Pt and Pd have very similar surface energies, the segregation energy is found to be very low. The segregation energy is given as the energy difference between two slabs with solute atoms in neighboring layers.

The segregation energy is positive and decays when moving the atoms deeper in the bulk. Already in the second sub-surface layer, the atoms no longer feel the influence of the surface and the segregation energy is negligible. The surface segregation is driven by lower surface energy of Au atoms compared to Pt and Pd. In total there are four different effects on the OH

adsorption energy: I) *surface ligand*, II) *sub-surface ligand*, III) *strain* and IV) *geometric* effects.

The presence of Au is found to be able to increase the catalytic activity over the pure PtPd alloys. In the case of PtPd and PtAu, the *surface ligand* effect increases the binding energy (BE) of OH, when the Pd or Au content on the surface is increased. For Pd-Au on Pt (Figure 1b), the BE decreases substantially with the surface Pd content (by 0.4 eV when going from 100% Pd to 67% Au on the surface). This behavior is complex and cannot be explained by, e.g., a simple *d*-band model.

The *sub-surface ligand effect* of e.g. Au in PdAu on Pt always decrease the BE of OH. The *strain effect* is found to be limited for the PtPd alloys because of very similar lattice constants for Pt and Pd, whereas the strain effect is higher in the Au-containing systems.

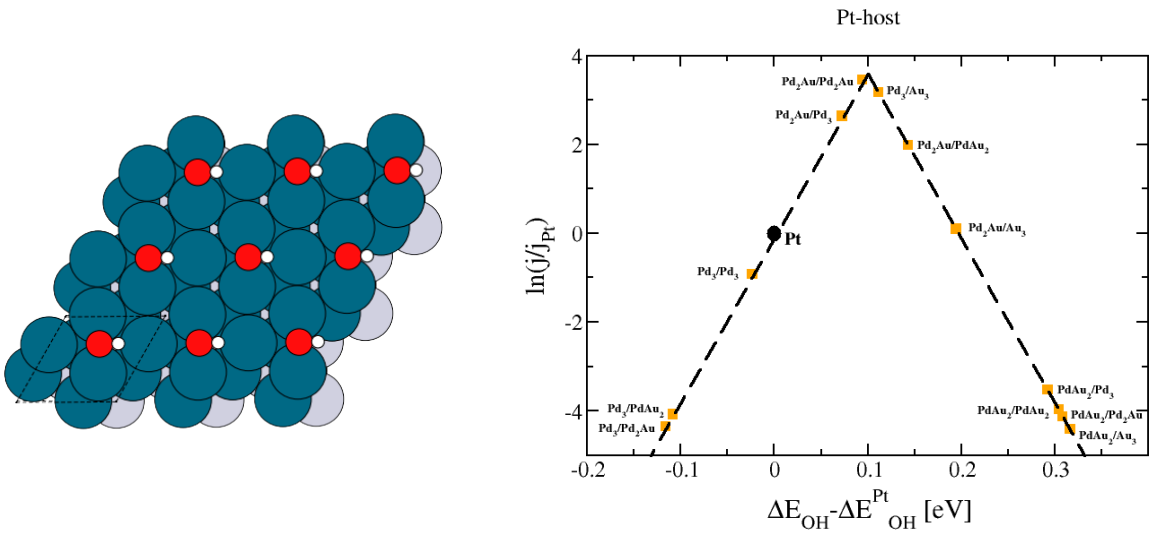


*Figure 1 a) Model system for studying the effect on the OH-binding energy of varying the surface composition in the two topmost layers (blue) on a fixed core (grey). b) ORR activity of Pd/Au on a fixed Pt-core.*

*The geometric effect* is seen in certain mixtures, because the adsorption site of OH changes as a function of the metal content in the surface layer. This effect can vary from small, e.g. the energy difference between the fcc and bridge sites, to very large, where OH is forced to be in the least preferred on-top sites.

Overall, a range of promising bi- and tri-metallic compositions yield higher ORR activity than Pt(111). Attaining favorable activities can be achieved through the combination of the 4 mentioned effects and the Pd-Pt-Au system was therefore selected for systematic investigations in the different core-shell nanoalloy configurations.

## 1.2 Core-shell nanoparticles

DFT calculations were performed on 309-atom icosahedral clusters utilizing the LCAO implementation of the GPAW 0.10 code [https://wiki.fysik.dtu.dk/gpaw/] and the RPBE exchange correlation functional along with a double-zeta basis set was employed. The focus of these calculations was to quantify the strain and ligand effects in the alloyed Au, Pd and Pt icosahedral nanoparticles (Figure 2), as these have shown interesting ORR properties [7]. Initially, geometry relaxations were performed on the pure clusters, following this, relaxations were undertaken on the complete core-shell $A_{162}B_{147}$ clusters. To investigate strain effects, the core-shell alloyed clusters were transformed to monometallic systems and single point energies calculated without any geometric relaxation ($A_{309}B_{\{xyz\}}$).

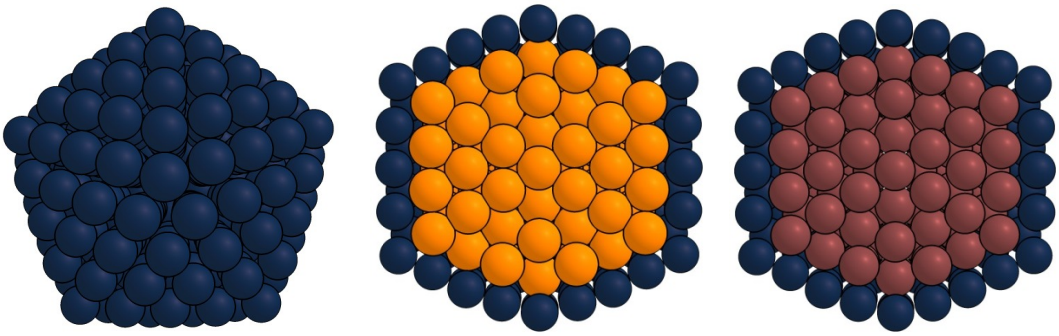

*Figure 2: Schematic showing pure and a cross-section of core-shell particles. (Left) $Pt_{shell}Pt_{core}$, (middle) $Pt_{shell}Au_{core}$ and (right) $Pt_{shell}Pd_{core}$.*

The size mismatch between the three atom types is negligible 169, 174 and 177 pm for Au, Pd and Pt, respectively. The root mean squared displacement (RMSD) was used to determine geometric displacements through alloying. RMSD is defined as in Eq. (1.1).

$$RMSD = \sqrt{\frac{1}{N}\sum_i^N m_i - m_i^*} \qquad (1.1)$$

*N* is the total number of atoms, $m_i$ is the position of a given atom for the relaxed pure particle and $m_i^*$ is the position of the same atom in the relaxed alloyed particle. Prior to applying this equation, rotation and translation operators were performed to align each particle, thereby minimizing the RMSD.

The average RMSD for the whole particle gives an indication of the extent to which a particle is distorted. This is larger for e.g. the $Au_{shell}Pd_{core}$ than $Au_{shell}Pt_{core}$ particles, meaning there is less distortion of the $Au_{shell}Pt_{core}$ (relative to the $Au_{309}$ particle), compared with the $Au_{shell}Pd_{core}$. In each case, it was found that there was greater displacement of shell atoms compared to the core. This is to be expected, as the coordination of the shell atoms is less than that of the core atoms meaning there will be displaced more easily.

These effects are shown by a representative cross-section of the particle, coloured according to atomic displacement, relative to the $Au_{309}$ particle (Figure 3). Here, it is apparent that there are clear differences between which atoms are displaced when comparing the $Au_{shell}Pd_{core}$ and $Au_{shell}Pt_{core}$ particles. This is of particular interest when different displacements are

observed for the shell atoms, which will have an effect on the catalytic activity of the particle through altering facet sites.

Comparing the relaxed and constrained pure structures, there was a greater energetic penalty associated with the constrained $Au_{309}Pd_{\{xyz\}}$ compared to the $Au_{309}Pt_{\{xyz\}}$ geometry. This ordering is to be expected from the RMSD values, where greater displacement is found for the AuPd particle. For AuPd and AuPt, the energetic penalty is the result of compressive strain on the Au shell, leading to a slight reduction in the diameter of the cluster.

Following the investigation of strain, ligand and geometric effects were investigated. Ten symmetry in-equivalent binding sites were investigated for the pure (relaxed and constrained) as well as the core-shell (relaxed) clusters, as shown in Figure 3 (Right). This approach enabled us to investigate shift in, e.g. the preferred adsorption sites for atomic oxygen.

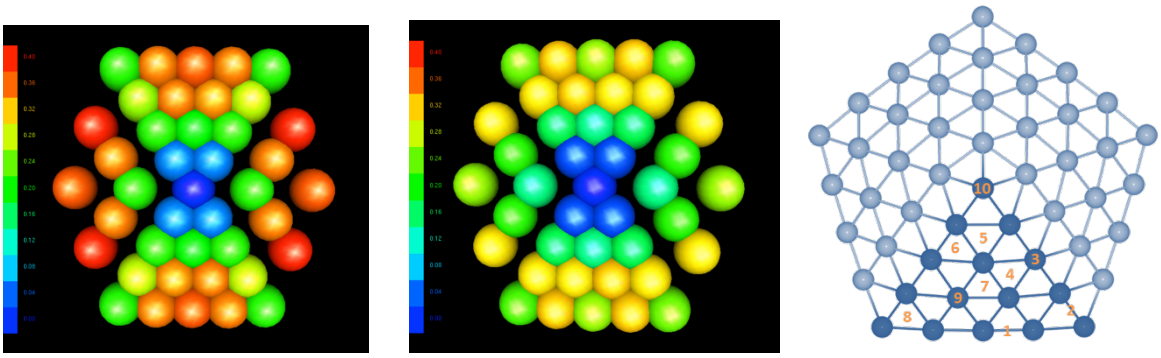


*Figure 3: Visual representations of atomic distortions for $Au_{shell}Pd_{core}$ (Left) and $Au_{shell}Pt_{core}$ (Middle). Root mean squared displacement (RMSD) are plotted as a function of colour, where blue shows little displacement and red shows large displacement. (Right) The 10 symmetry in-equivalent O and OH-binding sites investigated.*

There is generally stronger binding to the Pd surface, than the Au surface, although this is not the case for all sites. This shows that strain inherent in the alloyed particle leads to a weakening of oxygen binding; however, this effect is outweighed by the electronic effects, where the presence of a Pd core leads to significantly stronger Au-O binding. There is a significant difference due to electronic effects, induced by alloying, for the Au-rich clusters. However, for e.g. the Pd-rich clusters, when comparing the $Pd_{309}$ and $Pd_{162}Au_{147}$, there is generally less of a significant difference.

## 2 Summary

The Pt-Pd-Au system shows promising results and demonstrates some fundamental differences for the Pt-Pd-Au icosahedral nanoparticle and thin-film systems, which are of significant importance in understanding the catalytic ORR activity and stability. This work has now been extended to include the use of genetic algorithms [8] to predict the structural stability and activity of the alloyed nanoparticle catalysts under operating conditions.

# 3 References

1. P. Strasser et al., *Lattice-strain control of the activity in dealloyed core–shell fuel cell catalysts*, Nature Chemistry 2, 454 (2010).
2. J. Greeley et al., *Alloys of platinum and early transition metals as oxygen reduction electrocatalysts*, Nature Chemistry 1, 552 (2009).
3. W. Liu et al*., Bimetallic Aerogels: High-Performance Electrocatalysts for the Oxygen Reduction Reaction,* Angew. Chem. Int. Ed. 52, 1 (2013).
4. I, E. L. Stephens, A. S. Bondarenko, L. Bech, I. Chorkendorff, *Oxygen Electroreduction Activity and X-Ray Photoelectron Spectroscopy of Platinum and Early Transition Metal Alloys*, ChemCatChem 4, 341 (2012).
5. K. Sasaki, H. Naohara, Y. Choi, Y. Cai, W.-F. Chen, P. Liu, R. R. Adzic*, Highly stable Pt monolayer on PdAu nanoparticle electrocatalysts for the oxygen reduction reaction*, Nature Communication 3, 1115 (2012).
6. H.-Y. Park et al*., Enhancement of oxygen reduction reaction on PtAu nanoparticles via CO induced surface Pt enrichment,* Applied Catalysis B: Environmental 129, 375 (2013).
7. J. Wu, L. Qi, H. You, A. Gross, J. Li, H. Yang*, Icosahedral Platinum Alloy Nanocrystals with Enhanced Electrocatalytic Activities*, J. Am. Chem. Soc. 134, 11880 (2012).
8. S. Lysgaard, D.D. Landis, T. Bligaard, T. Vegge*, Genetic algorithm procreation operators for alloy nanoparticle catalysts,* Topics in Catalysis 57, 33 (2014).